


An Engineered Complement Factor H Construct for Treatment of C3 Glomerulopathy

Yi Yang,¹ Harriet Denton,¹ Owen R. Davies,² Kate Smith-Jackson,¹ Heather Kerr,³ Andrew P. Herbert,³ Paul N. Barlow,³ Matthew C. Pickering,⁴ and Kevin J. Marchbank¹ 

¹Institute of Cellular Medicine, Newcastle University and National Renal Complement Therapeutics Centre, Royal Victoria Infirmary, Newcastle upon Tyne, UK; ²Institute for Cell and Molecular Biosciences, Newcastle University, Newcastle upon Tyne, UK; ³Department of Chemistry, Edinburgh University, Edinburgh, UK; and ⁴Department of Medicine, Imperial College London, London, UK

ABSTRACT

Background C3 glomerulopathy (C3G) is associated with dysregulation of the alternative pathway of complement activation, and treatment options for C3G remain limited. Complement factor H (FH) is a potent regulator of the alternative pathway and might offer a solution, but the mass and complexity of FH makes generation of full-length FH far from trivial. We previously generated a mini-FH construct, with FH short consensus repeats 1–5 linked to repeats 18–20 (FH^{1–5^18–20}), that was effective in experimental C3G. However, the serum $t_{1/2}$ of FH^{1–5^18–20} was significantly shorter than that of serum-purified FH.

Methods We introduced the oligomerization domain of human FH-related protein 1 (denoted by R1–2) at the carboxy or amino terminus of human FH^{1–5^18–20} to generate two homodimeric mini-FH constructs (FH^{R1–2^1–5^18–20} and FH^{1–5^18–20^R1–2}, respectively) in Chinese hamster ovary cells and tested these constructs using binding, fluid-phase, and erythrocyte lysis assays, followed by experiments in FH-deficient *Cfh*^{–/–} mice.

Results FH^{R1–2^1–5^18–20} and FH^{1–5^18–20^R1–2} homodimerized in solution and displayed avid binding profiles on clustered C3b surfaces, particularly FH^{R1–2^1–5^18–20}. Each construct was >10-fold more effective than FH at inhibiting cell surface complement activity *in vitro* and restricted glomerular basement membrane C3 deposition *in vivo* significantly better than FH or FH^{1–5^18–20}. FH^{1–5^18–20^R1–2} had a C3 breakdown fragment binding profile similar to that of FH, a >5-fold increase in serum $t_{1/2}$ compared with that of FH^{1–5^18–20}, and significantly better retention in the kidney than FH or FH^{1–5^18–20}.

Conclusions FH^{1–5^18–20^R1–2} may have utility as a treatment option for C3G or other complement-mediated diseases.

J Am Soc Nephrol 29: 1649–1661, 2018. doi: <https://doi.org/10.1681/ASN.2017091006>

The hallmarks of C3 glomerulopathy (C3G)¹ are uncontrolled activation of the alternative pathway complement activation and abnormal deposition of complement components within the glomerulus.^{1–3} C3G is often associated with defective function of factor H (FH) or FH-related proteins (FHR 1–5).^{4–6} Uncontrolled activation of complement leads to ESRD in >50% of patients with C3G within 10 years of diagnosis. Depending on histologic and molecular diagnoses, C3G can be categorized into dense deposit disease, C3 GN, and complement FHR protein 5 nephropathy.⁷ More recently, gain-of-function mutations in the

positive regulators of the alternative pathway such as FHR-1 and -5 have been identified that can also trigger C3G.^{8–10} FHR-1, FHR-2, and FHR-5 form

Received September 20, 2017. Accepted February 26, 2018.

Published online ahead of print. Publication date available at www.jasn.org.

Correspondence: Dr. Kevin J. Marchbank, Newcastle University, Institute of Cellular Medicine, 3rd Floor William Leech Building, The Medical School, Framlington Place, Newcastle upon Tyne NE1 7RU, UK. Email: kevin.marchbank@newcastle.ac.uk

Copyright © 2018 by the American Society of Nephrology

homodimers and heterodimers through their first two N-terminal domains^{11,6}; the resulting dimers compete with FH for C3b binding, fine-tuning FH function on self and nonself surfaces.^{12,13}

FH and the FHRs share a common structure in the form of a string of short consensus repeat (SCR) domains (also known as sushi or complement control protein domains).¹⁴ FH, the most important serum alternative pathway regulator,¹⁵ is highly glycosylated.¹⁶ It displays both decay-accelerating activity, rapidly disrupting C3bBb, and cofactor activity (CFA) for factor I (FI)-mediated cleavage of C3b to iC3b.^{15,17,18} These functions map to the N-terminal SCRs 1–4.^{19–21} The actions of FH are directed to self-cells *via* interactions with glycosaminoglycans (GAGs),^{22–26} sialic acid,²⁷ or C3 fragments.^{19–21,23,24} For instance, the C-terminal SCRs 19–20 help to target FH to the glomerular basement membrane (GBM) *via* GAGs and C3d(g).^{28,29}

C57BL/6 mice with homozygous deficiency of FH (*Cfh*^{−/−}) are a widely accepted experimental model of C3G.³⁰ Here, uncontrolled alternative pathway activation consumes complement, resulting in low plasma C3 and C5 levels and the spontaneous development of C3G. Pathologically, this is characterized by linear deposition of C3 and C9 along the GBM of the kidney,^{1–3,30} demonstrating the key role of complement and the membrane attack complex.³¹ Eculizumab, a humanized anti-C5 antibody, was recently approved in the United Kingdom for use post-renal transplant in patients with C3G, but treatment of patients with C3G with eculizumab has had mixed success.^{32,33} Use of drugs that block C3 activation are more likely to reduce renal injury and are under investigation in C3G.³⁴

The optimal anti-C3 therapeutic approach is unclear but injection of 3–6 nmol of plasma purified human or murine FH to *Cfh*^{−/−} mice restored the secondary complement deficiency and reduced glomerular C3 deposition.^{35,36} Replicating this in man, *i.e.*, using full-length plasma purified or recombinant FH, could work in FH-deficient patients but the size and glycosylation complexity of FH poses a great challenge for biopharmaceutical manufacturing to the quantities required.^{37–39} Consequentially, FH-derived recombinant fusion proteins have been generated.^{40–43} Among these was the Newcastle version of a minimal FH (FH SCR1–5 fused to SCR18–20, *i.e.*, FH^{1–5^18–20} aka mini-FH).^{41,43} This molecule ameliorates experimental C3G in *cfh*^{−/−} mice at a relatively high dose (12 nmol).⁴³ However, these mini-FH agents have a significantly reduced *in vivo* *t*_{1/2} (2–5 hours) when compared with FH.^{43–45} Here, we describe the generation and pharmacodynamic testing of two homodimeric mini-FH (FH^{R1–2^1–5^18–20} and FH^{1–5^18–20^R1–2}) agents that demonstrate significantly improved complement regulatory function and serum *t*_{1/2} when compared with FH^{1–5^18–20} in the experimental model of C3G.³⁰

Significance Statement

Treatment options for C3 glomerulopathy (C3G, also called dense deposit disease or MPGN II) are limited. Supplement of factor H (FH, a potent complement regulator) in both murine models and patients can ameliorate disease. However, production of sufficient quantities of FH has proved challenging. Recombinant minimal versions of FH (mini-FH) possess improved complement regulatory function and are readily produced in culture but their serum *t*_{1/2} is approximately 1.5 hours in animal models. By introduction of an FH-related protein dimerization module to mini-FH, the authors have significantly improved complement regulatory function and serum *t*_{1/2} (approximately 9 hours). This approach represents a practical solution to improving anticomplement drug function and, importantly, could eventually provide a viable treatment for patients with complement-mediated diseases, particularly C3G.

METHODS

Construct Design

The two HDM-FH expression vectors were generated by standard domain shuffling techniques using our in-house vectors.⁴³ Please see the Supplemental Material for full details. All newly generated constructs were sequence verified and transfected into Chinese hamster ovary cells using jetPEI (Polyplus; VWR, Leicestershire, UK) following the manufacturer's protocols and as previously described.^{41,43} Extinction coefficients and the theoretic molecular masses of monomeric FH^{R1–2^1–5^18–20} (ϵ : 124,660; molecular mass: 70,944 Da) and FH^{1–5^18–20^R1–2} (ϵ : 124,660; molecular mass: 71,132 Da) secreted proteins were calculated using ExPASy ProtParam program (Swiss Institute of Bioinformatics, Lausanne, Switzerland).

Size Exclusion Chromatography Multiangle Light Scattering

Size exclusion chromatography multiangle light scattering (SEC-MALS)⁴⁶ was performed using an ÄKTA Pure with a Superdex 200 Increase 10/300 GL column (GE Healthcare), with in-line DAWN HELEOS II MALS detector (eight fixed angles) and Optilab T-REX differential refractometer (Wyatt Technology). Protein samples (100 μ l of 0.5–2.0 mg/ml) were analyzed in PBS buffer running at 0.5 ml/min. Data were collected and analyzed using ASTRA 6 (Wyatt Technology). Molecular masses were calculated across eluted protein peaks through extrapolation from Zimm plots using a *dn/dc* value of 0.1850 ml/g. Protein conjugation analysis was performed through Zimm plot extrapolation using *dn/dc* values of 0.1850 ml/g and 0.1500 ml/g for protein and glycosyl groups, respectively, and protein UV extinction coefficients of 1.787 ml/mg per centimeter and 1.781 ml/mg per centimeter for FHR1–2^1–5^18–20 and FH1–5^18–20^R1–2, respectively.

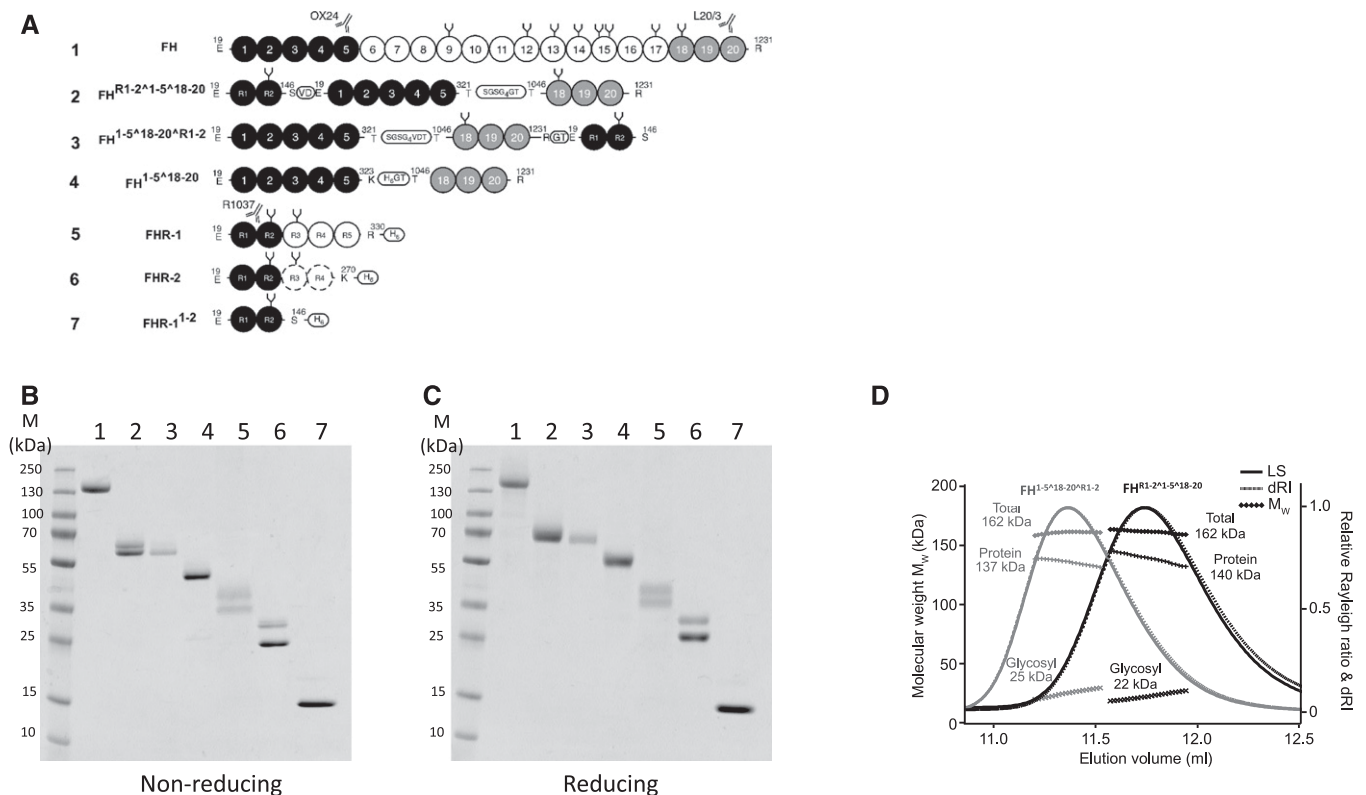


Figure 1. New mini-FH molecules dimerize in solution. (A) The FH family of proteins and derived recombinant proteins comprise SCR domains, which are represented by gray-scaled ovals to indicate the natural source of the module and their biochemical function. Constructs are numbered (1–7) and correspond to the lane identifiers in the analysis shown in (B) and (C). The amino acid sequences are on the basis of the UniProt database (FH accession no. P08603; FHR-1 accession no. Q03591; FHR-2 accession no. P36980) with single letter code used in the protein segments that have been shuffled into the recombinant constructs. Artificial linker sequences are indicated by boxes and glycosylation sites are indicated by black forks. mAb epitopes are indicated; OX24 and L20/3 antibodies recognize FH SCR 5 or SCR 20, respectively, whereas R1037 (a mouse mAb produced in-house against recombinant FHR1) recognizes FHR-1 SCR 1–2. (B) A nonreducing and (C) reducing 10%–20% gradient SDS-PAGE comparison of plasma purified human FH and recombinant FH^{1-5^18-20}, FH^{R1-2^1-5^18-20}, FH^{1-5^18-20^R1-2}, and all other control proteins. (D) SEC-MALS analysis of FH^{R1-2^1-5^18-20} (black) and FH^{1-5^18-20^R1-2} (gray). Molecular mass analysis (assuming unmodified proteins) reveals that FH^{R1-2^1-5^18-20} and FH^{1-5^18-20^R1-2} are dimeric species of 162 kD (approximately 22 kD sugar and approximately 140 kD protein), respectively. Light scattering (LS) and differential refractive index (dRI) are shown as solid and dashed lines, respectively, with fitted molecular masses (M_w) plotted as diamonds across elution peaks.

Binding Studies of FH-Derived Regulators

Protein interactions were analyzed by surface plasmon resonance (SPR) technology using a Biacore X100 (GE Healthcare) based on methods previously described.^{10,47} Full details may be viewed in the Supplemental Material.

Sheep Erythrocyte-Based Hemolytic Assays

- The antibody-mediated FH loss-of-function assay was carried out as previously described by Nichols *et al.*⁴³
- Decay-accelerating activity (DAA) and FI cofactor activity (CFA) of FH reagents on sheep erythrocyte surface were assessed using a method described previously by Tortajada *et al.*⁴⁸ with minor modifications. Please refer to the Supplemental Material.

Administration of Plasma Purified FH, FH^{1-5^18-20}, FH^{R1-2^1-5^18-20}, and FH^{1-5^18-20^R1-2} to *Cfh*^{-/-} Mice

Mice were housed at the Comparative Biology Centre, Newcastle University and all experiments were conducted in accordance with institutional guidelines and approved by the UK Home Office. All reagents were buffer exchanged into PBS and LPS was removed as previously described.⁴³ An identical volume (500 μ l) of plasma purified FH (3 nmol), FH^{1-5^18-20} (6 nmol), FH^{R1-2^1-5^18-20} (3 nmol of dimer), and FH^{1-5^18-20^R1-2} (3 nmol of dimer) or PBS was administered intraperitoneally to *Cfh*^{-/-} mice. Seven days before and at various time points during the experiment, blood samples were collected into EDTA *via* tail venesection and immediately placed on ice. Plasma was collected after centrifugation at 800 \times g for 10 minutes

and cell-free component stored at -80°C . At the end of the experiment, mice were euthanized (terminal exsanguination under anesthesia) and the kidneys were collected and snap frozen in liquid nitrogen prechilled isopentane. Tissue was stored at -80°C until required. Analysis of serum C3/FH and IHC was carried out essentially as previously described.⁴³ Please see the Supplemental Material for additional details.

RESULTS

Generation of Homodimeric Mini-FH ($\text{FH}^{\text{R1-2}\wedge\text{1-5}\wedge\text{18-20}}$ and $\text{FH}^{\text{1-5}\wedge\text{18-20}\wedge\text{R1-2}}$)

One potential problem of using $\text{FH}^{\text{1-5}\wedge\text{18-20}}$ in patients is its short serum $t_{1/2}$.²³ We sought a unique solution to this problem through the introduction of the first two N-terminal SCRs of FHR-1 (denoted R1–2) to $\text{FH}^{\text{1-5}\wedge\text{18-20}}$. This was principally on the basis of the fact that SCRs 1–2 of FHR-1 are primarily involved in dimerization of FHR1^{11,13} and that, when in isolation, did not interact with C5 or C3b, as previously shown (in the Supplemental Material)¹¹ using SPR.⁴⁹ Indeed, we also found no intrinsic complement regulatory or deregulatory function within this region using standard complement assays (see Supplemental Figures 5 and 6). Being mindful that fusion of SCR domains to Fc domains, to make them bivalent and long-lived, can also completely abrogate function,⁵⁰ we opted to attach SCRs 1–2 of FHR-1 to either the N or C terminus of $\text{FH}^{\text{1-5}\wedge\text{18-20}}$, generating $\text{FH}^{\text{R1-2}\wedge\text{1-5}\wedge\text{18-20}}$ and $\text{FH}^{\text{1-5}\wedge\text{18-20}\wedge\text{R1-2}}$, respectively (Figure 1A). This also allowed any effects of steric hindrance due to dimerization to be evaluated in an unbiased fashion. SDS-PAGE analysis indicated that homodimeric mini-FH constructs and control proteins could be purified from CHO culture to homogeneity (Figure 1, B and C). Proteins were readily detected by specific mAbs in western blot analysis, suggesting correct folding of both $\text{FH}^{\text{R1-2}\wedge\text{1-5}\wedge\text{18-20}}$ and $\text{FH}^{\text{1-5}\wedge\text{18-20}\wedge\text{R1-2}}$ (Supplemental Figure 1A). Noticeably, the SDS-PAGE profiles of $\text{FH}^{\text{R1-2}\wedge\text{1-5}\wedge\text{18-20}}$ and $\text{FH}^{\text{1-5}\wedge\text{18-20}\wedge\text{R1-2}}$ suggest that the constructs were differentially glycosylated as is common for FHR-1,⁵¹ with $\text{FH}^{\text{R1-2}\wedge\text{1-5}\wedge\text{18-20}}$ being split 50:50 between a two- and three-glycan isoform, confirmed by deglycosylation using PNGase F (Supplemental Figure 1B). Using traditional size exclusion chromatography with mixtures of FH and $\text{FH}^{\text{R1-2}\wedge\text{1-5}\wedge\text{18-20}}$ or $\text{FH}^{\text{1-5}\wedge\text{18-20}\wedge\text{R1-2}}$ these molecules elute in the same fractions, suggesting successful dimer formation (Supplemental Figure 2). This was confirmed using SEC-MALS, as used in the original description of the FHR1 dimerization domain.¹¹ SEC-MALS demonstrated total molecular masses for homodimeric mini-FH molecules as 160 ± 4 kD, estimated as 137–140 kD protein in dimers (consistent with the predicted size of the dimeric protein backbone) conjugated to approximately 22–25 kD of glycosyl groups, respectively (Figure 1D, Supplemental Figure 1C). This mass of glycosylation is consistent with a previous analysis of FH glycosyl composition.¹⁶ The increased mass noted for $\text{FH}^{\text{R1-2}\wedge\text{1-5}\wedge\text{18-20}}$

using SEC-MALS is likely a reflection of the higher percentage of the three-glycan isoform versus that noted for $\text{FH}^{\text{1-5}\wedge\text{18-20}\wedge\text{R1-2}}$ (Figure 1B). Recent data have indicated that FHR proteins can swap dimeric partner.⁵² To investigate if this would be an issue for the homodimeric mini-FH compounds, we assessed the ability of recombinant FHR1 or FHR2 to crosshybridize with homodimeric mini-FH. Although our data indicate FHR1 and FHR2 can crosshybridize in fluid-phase assay systems, particularly when FHRs are in abundance (and preferentially with the N-terminal dimer in certain circumstances), FHR1/2 crosshybridization is very low when carried out after homodimeric mini-FH binds to a C3b-coated surface (Supplemental Figures 3 and 4). FHR5 did not crosshybridize with either construct (Supplemental Figure 4).

Alternative Pathway Regulation by Homodimeric Mini-FH Constructs Compared with that of $\text{FH}^{\text{1-5}\wedge\text{18-20}}$ and Serum-Derived FH

We tested whether the homodimeric mini-FH molecules show modified C3 regulatory properties in fluid phase compared with FH and $\text{FH}^{\text{1-5}\wedge\text{18-20}}$. We incubated C3b with FI and a decreasing concentration of test reagent at 37°C and, after 1 hour, the quantity of C3b cleavage products ($\text{C3}\alpha'$ -68, -46, and -43) was investigated using SDS-PAGE. The assays demonstrated that the CFA of $\text{FH}^{\text{1-5}\wedge\text{18-20}\wedge\text{R1-2}}$ in the fluid phase was consistently approximately 50% greater than that of FH, whereas $\text{FH}^{\text{R1-2}\wedge\text{1-5}\wedge\text{18-20}}$ was comparable to FH and $\text{FH}^{\text{1-5}\wedge\text{18-20}}$ demonstrated a $>50\%$ reduced CFA (Figure 2); control proteins had no detectable complement regulatory function, as expected (Supplemental Figure 5).

Both Homodimeric Mini-FH Molecules Bind Tighter than Mini-FH to C3 Fragments and Heparin Sulfate

Using SPR, we qualitatively compared the ability of the homodimeric mini-FH constructs, mini-FH, and plasma purified FH to bind to C3-activation fragments, *i.e.*, C3b, iC3b, and C3d(g). First, we assessed binding of these reagents to a CM5 chip coated with 650 RUs of C3b, deposited in an orientation mimicking natural opsonization.^{10,47,53} Under these conditions, both homodimeric mini-FH constructs displayed avid binding kinetics as demonstrated by a prolonged dissociation phase (Figure 3A, Supplemental Table 1). Indeed, the very tight binding of the homodimeric mini-FH constructs meant we needed to use 40-fold less homodimeric mini-FH (at maximal concentration) than that commonly used in FH kinetic studies (normally start at $10\text{ }\mu\text{M}$,^{40,45,54}), hence the low RU values noted for FH. Additionally, and unfortunately, the heterogeneous binding profiles of the homodimeric mini-FH constructs prevent accurate K_D determination and traditional kinetic analysis. However, in repeat analysis, comparing the relative binding response of the four analytes at a single concentration of 125 nM (Figure 3C), $\text{FH}^{\text{R1-2}\wedge\text{1-5}\wedge\text{18-20}}$ gave the strongest binding signal followed by $\text{FH}^{\text{1-5}\wedge\text{18-20}\wedge\text{R1-2}}$, $\text{FH}^{\text{1-5}\wedge\text{18-20}}$, and FH. On the same CM5 chip converted to an iC3b surface (see the Supplemental Material⁴⁷),

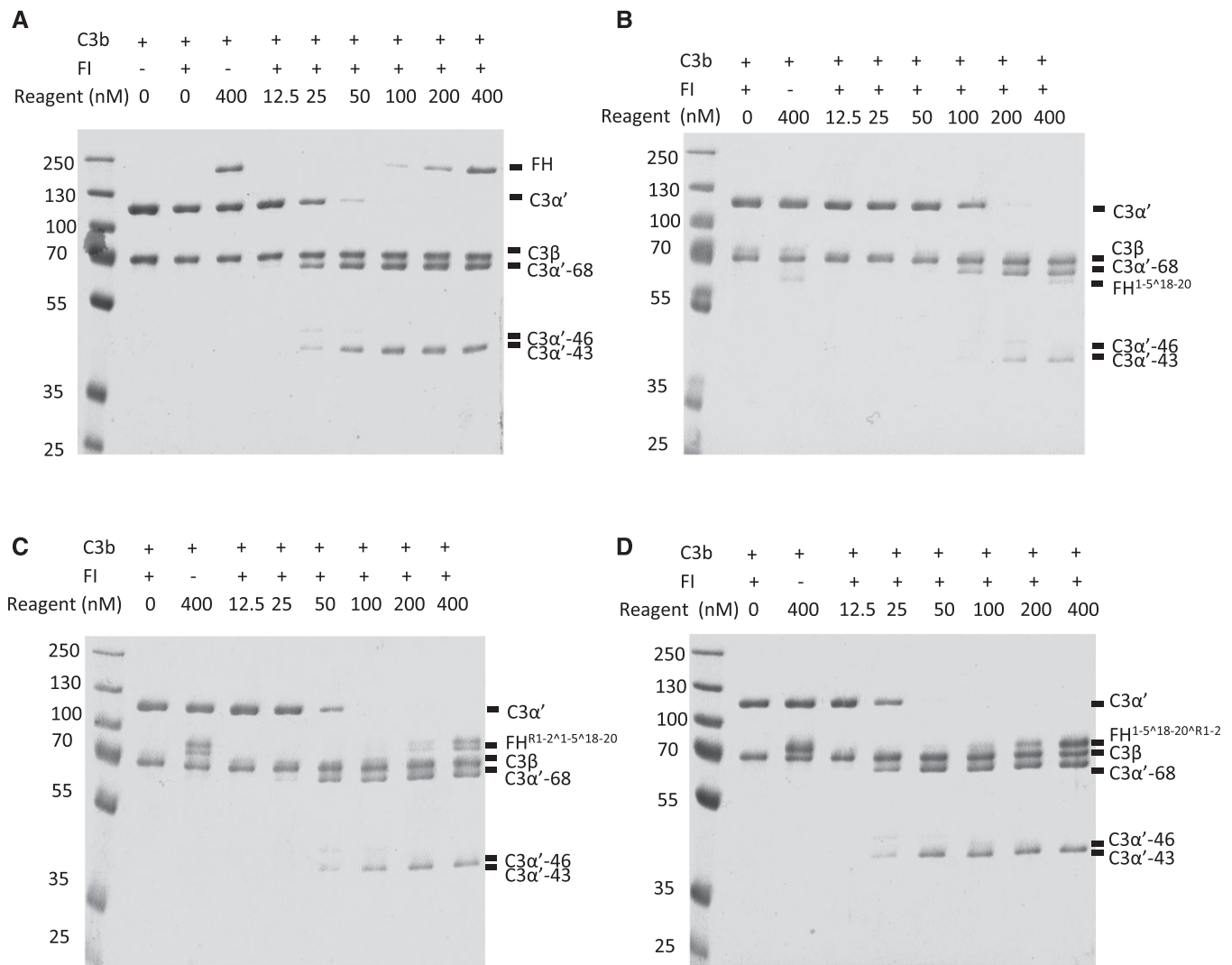


Figure 2. Compared to FH, HDM-FH constructs demonstrated improved or comparable fluid-phase cofactor activity. C3b (700 nM), FI (20 nM), and increasing concentrations of (A) FH, (B) FH^{1-5^18-20}, (C) FH^{R1-2^1-5^18-20}, or (D) FH^{1-5^18-20^R1-2} were incubated in solution at 37°C for 1 hour. C3b breakdown was analyzed by SDS-PAGE and Coomassie staining. Disappearance of C3α'-110 band and the appearances of C3α'-68, -46, and -43 bands were indicative of the C3b proteolytic inactivation. One experiment, representative of two independent experiments, is shown.

both homodimeric mini-FH constructs and FH^{1-5^18-20} bound with rapid on- and off-rates. On the iC3b surface, FH^{1-5^18-20^R1-2} demonstrated the highest binding response followed by FH^{R1-2^1-5^18-20} and FH^{1-5^18-20} (Figure 3B). On a separate CM5 chip with amine-coupled C3d (800 RUs),⁵⁵ FH^{R1-2^1-5^18-20} produced the strongest binding response to this surface, followed by FH^{1-5^18-20} and FH^{1-5^18-20^R1-2} (Figure 3D). These data suggest the “open” conformation of FH^{1-5^18-20} is maintained in the homodimeric mini-FH molecules compared with the “folded-back” conformation associated with full-length FH.^{14,55}

Protection of Host-Like Surfaces

The ability of FH to distinguish between self, foreign, and aberrant cells relies on targeting of FH by surface-tethered

C3-activation fragments and surface GAGs.^{13,22-27} As demonstrated above, the ability to bind C3-activation fragments was largely preserved in the homodimeric mini-FH constructs. We next assessed whether these new constructs had impaired GAG-binding using a heparin column as a chemical analog of GAGs. Interestingly, FH^{R1-2^1-5^18-20} demonstrated longer retention than FH^{1-5^18-20^R1-2} and both homodimeric mini-FH constructs eluted at a higher ionic strength than FH but at a lower ionic strength than FH^{1-5^18-20} (Figure 3E). These data suggest that the steric hindrance imparted on the homodimeric mini-FH constructs by the dimerization domains influences the ability of the GAG binding domains to bind heparin; as you would predict, this is most evident when the dimerization domain is attached to the C terminus of FH^{1-5^18-20}.

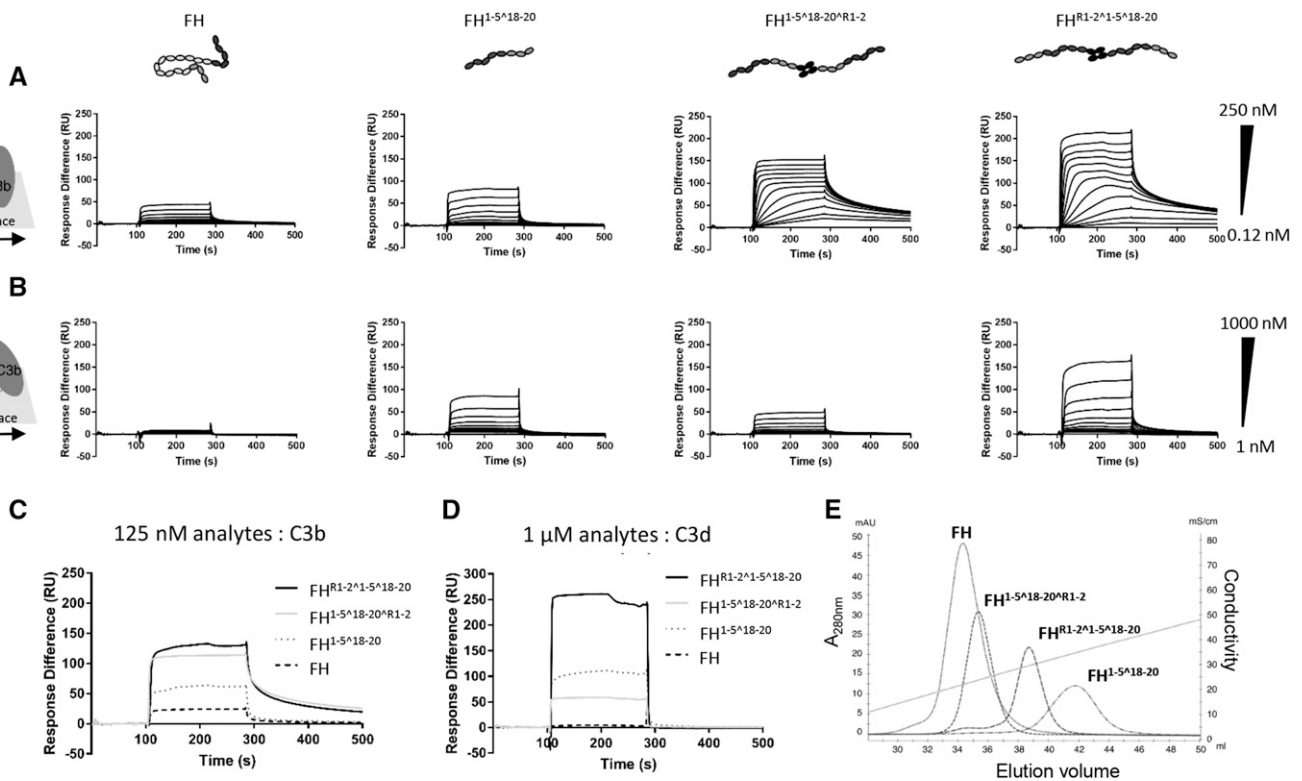


Figure 3. HDM-FH constructs bind with high avidity to their physiologic ligands. (A) Doubly diluted concentration series of FH, FH^{1-5Δ18-20}, FH^{R1-2Δ1-5Δ18-20}, or FH^{1-5Δ18-20ΔR1-2} were flowed over a C3 convertase deposited C3b chip at concentrations between 250 and 0.12 nM or (B) an iC3b chip at concentrations between 1000 and 1 nM. (C) Direct comparison of binding responses of FH, FH^{1-5Δ18-20}, FH^{R1-2Δ1-5Δ18-20}, and FH^{1-5Δ18-20ΔR1-2} at 125 nM on a C3 convertase deposited C3b chip. (D) Direct comparison of binding responses of FH, FH^{1-5Δ18-20}, FH^{R1-2Δ1-5Δ18-20}, and FH^{1-5Δ18-20ΔR1-2} at 1000 nM on a CM5 chip amine coupled with 650 RUs C3d. For all SPR experiments, one sensorgram of an experiment performed two times is shown. (E) The GAG binding strength of FH, FH^{1-5Δ18-20}, FH^{R1-2Δ1-5Δ18-20}, or FH^{1-5Δ18-20ΔR1-2} was analyzed by heparin chromatography. The conductivity of the elution peak indicates the binding strength to the chemical analog of the host surface polyanionic motifs. One chromatogram from two independent experiments is shown.

Next, we evaluated the homodimeric mini-FH constructs in hemolysis protection assays using human C3b-coated sheep erythrocytes, which also bear human-like sialic acid.⁵⁴ In agreement with previous data,⁴³ FH^{1-5Δ18-20} demonstrated marginally, but consistently, more potent decay accelerating and CFA *i.e.*, approximately two-fold when compared with FH (Figure 4, A and B, Supplemental Table 2). Strikingly, when compared with FH, FH^{1-5Δ18-20ΔR1-2} demonstrated 33- and 64-fold increases in decay accelerating and CFA on the basis of mean IC₅₀, respectively (Supplemental Table 2), whereas FH^{R1-2Δ1-5Δ18-20} demonstrated approximately 20-fold increases in both decay accelerating and CFA, respectively (Supplemental Table 2).

Mutations in FH and anti-FH autoantibodies are recognized as contributors to pathology in aHUS and C3G.^{56,57} Mutations in FH associated with aHUS are common in SCR 19–20 and result in reduced cell surface association.^{23,28} Reconstituting FH-depleted serum with a mutant recombinant FH (aHUS associated p.S1191A/p.V1197A; *i.e.*, the FHR1 reverse hybrid^{13,53}) provides a model system with which to test the

potential of therapies to reverse complement dysregulation. Using this approach, the homodimeric mini-FH constructs were found to be more potent than plasma purified FH in protection of sheep erythrocytes from hemolysis (Figure 4C), with FH^{R1-2Δ1-5Δ18-20} being the most potent (Supplemental Table 3). We have previously shown that the FH SCR-5 binding mAb OX-24 attenuates FH regulatory function in normal human serum providing a model system for anti-FH associated C3G.^{43,53} In this model, FH^{R1-2Δ1-5Δ18-20} was also consistently more potent in protecting sheep erythrocytes from hemolysis than either FH^{1-5Δ18-20ΔR1-2} or FH^{1-5Δ18-20} (Figure 4D). In order to assess the functional effect, if any, of the presence of FHR1 or -2 on the homodimer mini-FH or mini-FH constructs. We repeated the FH mutant protein assay either with or without a preincubation with FHR1 and FHR2 at physiologic concentrations. The addition of these proteins to the assay had no appreciable effect on function (Figure 5E, Supplemental Figure 6D, Supplemental Table 4).

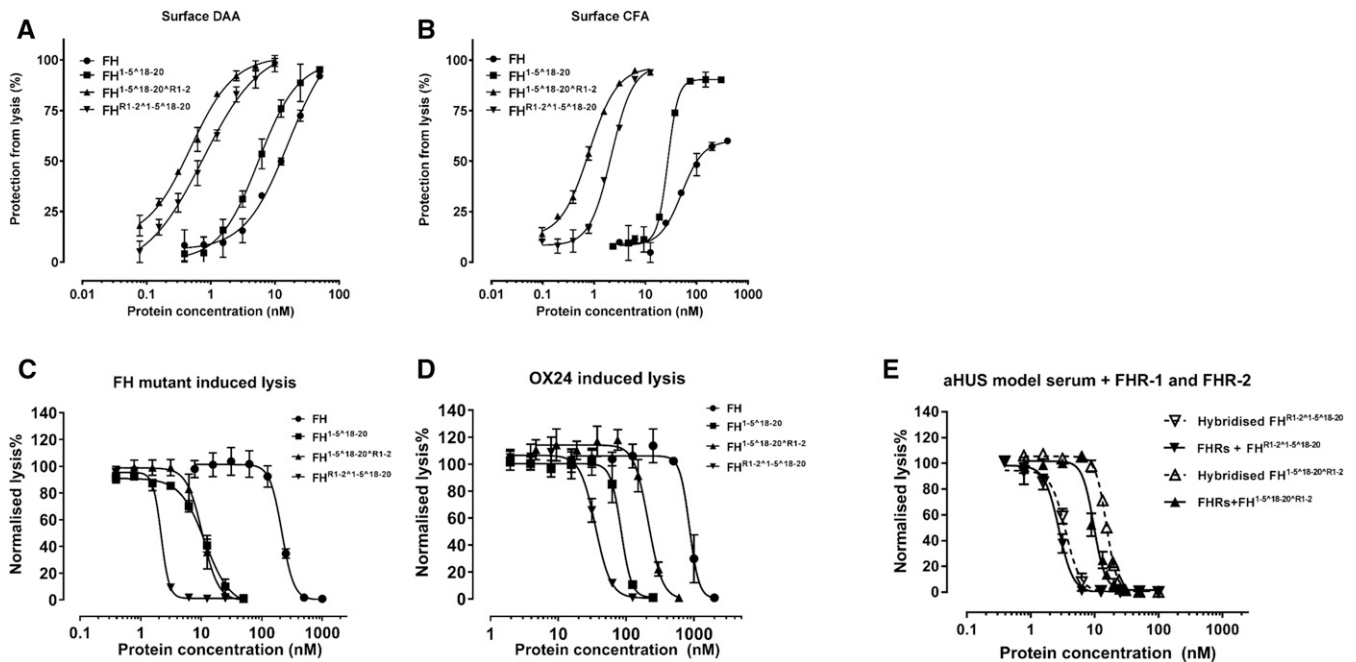


Figure 4. HDM-FH protects “host-Like” surfaces significantly better than FH. (A) Decay acceleration activity of FH reagents on surface-bound AP C3 convertase. C3 convertases were reconstituted on the surface of C3b as described in the Methods. The decay of the AP C3 convertases was accelerated by FH (●), FH^{1-5^18-20} (■), FH^{R1-2^1-5^18-20} (▼), and FH^{1-5^18-20^R1-2} (▲). The remaining AP C3 convertase activity was then determined by the amount of lysis of sheep erythrocyte after incubation with FB- and FH-depleted serum in PBS supplemented with 20 mM EDTA. (B) FI CFA of FH and its derivatives. The C3b precoated sheep erythrocytes were exposed to a concentration gradient of FH reagents together with 2.5 μ g/ml of FI. The remaining C3b molecules on the sheep erythrocyte surface bind FB (70 μ g/ml) and FD (0.4 μ g/ml) to form AP C3 convertase, which leads to cell lysis during incubation with FB- and FH-depleted serum in PBS supplemented with 20 mM EDTA. Plasma purified FH, FH^{1-5^18-20}, FH^{R1-2^1-5^18-20}, and FH^{1-5^18-20^R1-2} also protect sheep erythrocytes from lysis in human sera with deregulated complement AP. (C) The addition of increasing concentrations of FH reagents prevented sheep erythrocyte lysis in FH-depleted serum supplemented with recombinant human FH S1191A V1197L.²⁷ (D) The increasing concentrations of FH reagent, as indicated, protected sheep erythrocytes from AP-mediated lysis in OX24-spiked normal human serum (an autoantibody model serum²³). (E) The functional effects of potential heterodimer formation between homodimeric mini-FH and recombinant FHR were evaluated using a hemolytic assay essentially as described above. However, before serum was added, a concentration series of doubly diluted compounds, as indicated, were preincubated with either recombinant human FHR-1 and FHR-2 at physiologic serum concentration (solid line) or buffer alone (dashed line) for 1 hour. Sheep erythrocyte lysis was measured by the hemoglobin release (A_{405}). For (A) and (B), data were processed using 100% lysis determined in water and 0% lysis of diluted serum diluted in buffer alone, whereas for (C) and (D) the data were normalized against sheep erythrocyte lysis with deregulated sera in the absence of FH reagent. Six independent measurements of three experiments were shown, except for (A) and (B) that show data from three independent measurements of one experiment. The mean and SD for each measurement were calculated for all datasets; sigmoidal curves were fitted using nonlinear regression function in GraphPad Prism. aHUS, atypical Haemolytic uremic syndrome; DAA, decay accelerating activity; CFA, cofactor activity.

Homodimeric Mini-FH Constructs Display Extended Serum $t_{1/2}$ and Dramatically Reduce Glomerular C3 Staining in *Cfh*^{-/-} Mice

We next compared the *in vivo* C3 regulatory efficacy and pharmacodynamics of both homodimeric mini-FH constructs. *Cfh*^{-/-} mice received a single intraperitoneal injection of 3 nmol of FH^{R1-2^1-5^18-20}, FH^{1-5^18-20^R1-2}, or human plasma-derived FH, previously reported as an effective dose.³⁶ Herein, we also opted to use 6 nmol of FH^{1-5^18-20} as control. This is half the previously published effective dose⁴³ but allows us to control for the absolute number of FH SCR 1–5 domains injected into the mice. After

administration of a single dose of the homodimeric mini-FH constructs to FH-deficient mice, both reagents were detectable in the serum for up to 48 hours and demonstrated a similar β phase $t_{1/2}$ of approximately 8.4 hours. Despite this five-fold improved $t_{1/2}$ compared with that of FH^{1-5^18-20} (1.7 hours), it remains only 50% of the $t_{1/2}$ value of FH (17.5 hours; Figure 5A). As expected, FH^{1-5^18-20} only partially restored plasma C3 level at 2 hours postinjection (Figure 5B). In contrast, both homodimeric mini-FH constructs show an extended period of C3 restoration of up to 48 hours. Encouragingly, FH^{1-5^18-20^R1-2} demonstrated a complete restoration of plasma C3 level in the 24-hour sample (Figure 5B). This serum C3

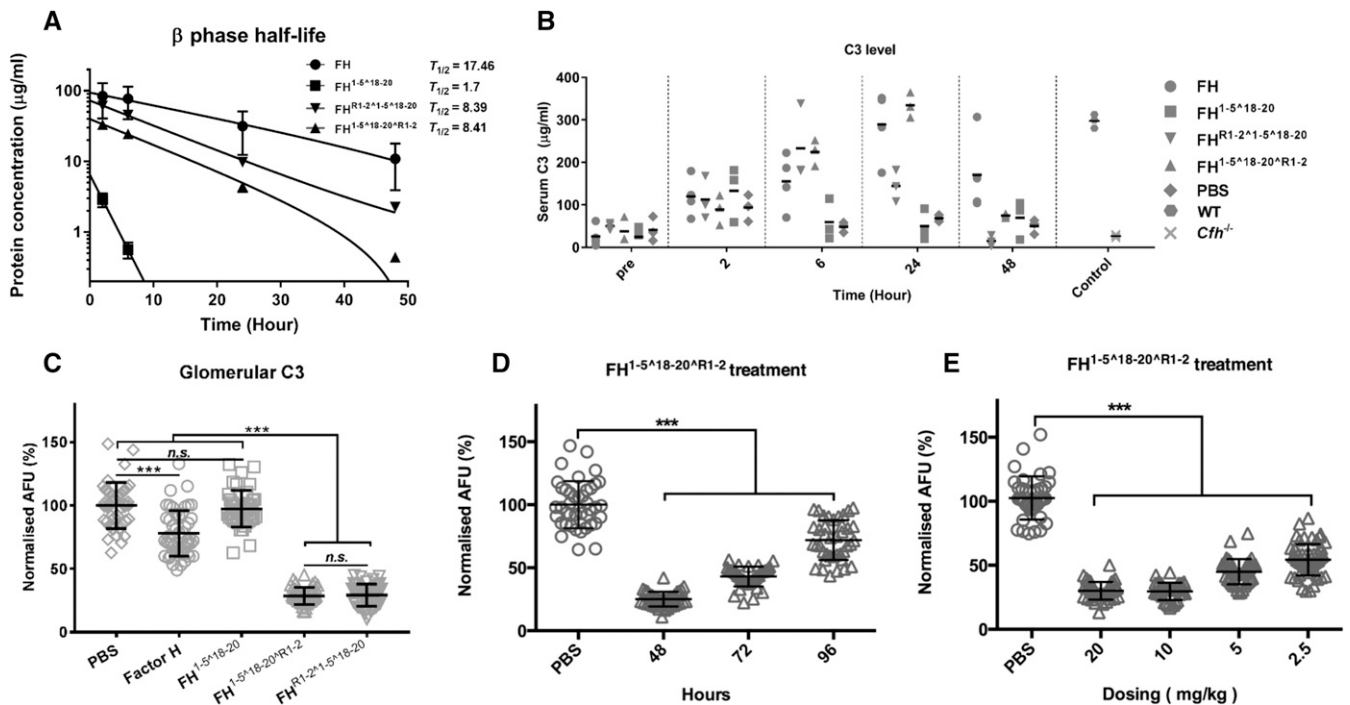


Figure 5. HDM-FH is highly effective in restoring intact C3 levels and reducing glomerular C3 deposits. Mice were dosed with 3 nmol plasma purified FH (●), $\text{FH}^{1-5\wedge 18-20}$ (■), $\text{FH}^{\text{R1-2}\wedge 1-5\wedge 18-20}$ (▼), and $\text{FH}^{1-5\wedge 18-20\wedge \text{R1-2}}$ (▲). (A) FH and its derivatives were detected in plasma collected at various intervals postinjection using an OX-24 and goat-anti-FH polyclonal-based ELISA. OD readings were converted to micrograms per milliliter. The data were fitted into natural log decay curves, plotted in log scale against time. (B) Plasma C3 levels were detected using mAb 11H9 to capture and a polyclonal anti-C3 to detect. OD450 readings were converted to micrograms per milliliter using purified mouse C3 as standard. (C) Quantitative analysis of glomerular C3 immunofluorescence intensity at 48 hours after a single injection of plasma purified human FH, $\text{FH}^{1-5\wedge 18-20}$, $\text{FH}^{\text{R1-2}\wedge 1-5\wedge 18-20}$, $\text{FH}^{1-5\wedge 18-20\wedge \text{R1-2}}$, or PBS. (D) Quantified glomerular C3 immunofluorescence intensities at 48, 72, or 96 hours after a single injection of $\text{FH}^{1-5\wedge 18-20\wedge \text{R1-2}}$ were compared with mice treated with PBS. (E) Glomerular C3 immunofluorescence intensities after a single injection of 20–2.5 mg/kg (approximately 3–0.375 nmol) $\text{FH}^{1-5\wedge 18-20\wedge \text{R1-2}}$ were compared with that treated with PBS at 48 hours. For (C–E), for every condition >40 glomeruli at $\times 10$ magnification from three mice were analyzed by ImageJ.⁴⁶ In (A), the mean and SD for each measurement were calculated for all data points; natural log exponential decay curves were used to calculate $T_{1/2}$ using GraphPad Prism. In (B), data are shown in a scatter dot plot; the black bar indicates the mean of each dataset. For (C–E), unpaired t test was performed as indicated. *** $P < 0.001$; n.s., $P > 0.05$. AFU, arbitrary fluorescent units; PBS, phosphate buffered saline; WT, wild-type.

restoration profile was broadly comparable to that of the plasma purified human FH.

C3 fragment deposition and FH retention in the kidney were analyzed by immunofluorescent staining. At 48 hours post-injection, C3 fragment deposits were significantly reduced in mice injected with homodimeric mini-FH constructs and FH, whereas $\text{FH}^{1-5\wedge 18-20}$ marginally reduced detectable C3 fragment deposits. An analysis of C3 fragment intensity, in >40 glomeruli, concluded that both homodimeric mini-FH constructs reduced detectable C3 deposits to almost background levels, significantly lower than FH or $\text{FH}^{1-5\wedge 18-20}$ (Figure 5C, Supplemental Figure 7). Furthermore, $\text{FH}^{1-5\wedge 18-20\wedge \text{R1-2}}$ could provide significant C3 reductions out to 96 hours (Figure 5D, Supplemental Figure 8B). We were also able to reduce the dose of $\text{FH}^{1-5\wedge 18-20\wedge \text{R1-2}}$ to 0.375 nmol or 2.5 mg/kg and achieve a significant reduction in glomerular C3 staining (Figure 5E, Supplemental Figure 8A). In our previous study, we

demonstrated that $\text{FH}^{1-5\wedge 18-20}$ and FH could be detected on the GBM 6 hours after administration.⁴³ Herein, and in contrast to FH, both homodimeric mini-FH constructs and $\text{FH}^{1-5\wedge 18-20}$ are detectable on the GBM at 24 hours, colocalizing with glomerular C3 fragments (Figure 6). Furthermore, $\text{FH}^{1-5\wedge 18-20\wedge \text{R1-2}}$ is still detectable, albeit faintly, at 48 hours after injection (Figure 6, right-hand panel).

DISCUSSION

Treatment options for C3G are an unmet clinical need. Minimal versions of FH (mini-FH constructs) could provide a solution if concerns about short serum $t_{1/2}$ can be negated. Here, we demonstrate that by forming dimers of $\text{FH}^{1-5\wedge 18-20}$, an enhanced *in vivo* pharmacodynamic and complement regulation profile can be obtained. Two differentially configured

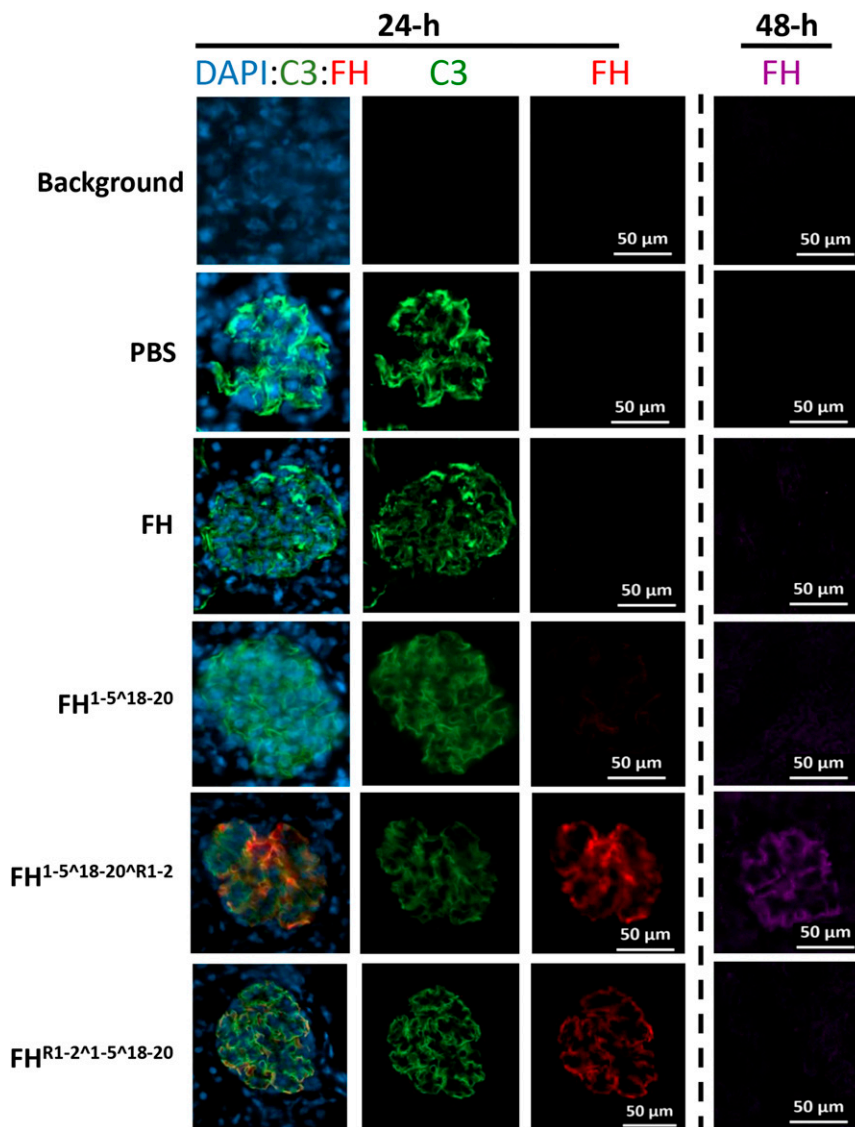


Figure 6. HDM-FH reduces C3 deposits and remains bound in the glomerulus for greater than 48hrs. Representative images are shown of mouse kidneys stained with a goat anti-mC3b-FITC (MP Biomedical) to detect glomerular C3 staining (green) and OX-24-Dylight 650 (generated in-house), which binds FH SCR5 (an integral epitope in all agents used in this experiment). OX-24 staining at 24 hours (red) or 48 hours (purple) after a single injection ip of the agent. Nuclei were stained with DAPI (blue). Original magnification, $\times 10$; a scale bar is shown. DAPI, 4',6-diamidino-2-phenylindole; PBS, phosphate-buffered saline.

homodimeric mini-FH molecules demonstrated subtly different alternative complement regulatory activities on the different assays applied, providing further insight into the rational design of therapeutic molecules derived from natural regulators.

The principal function of an FH-based drug is binding to C3b and regulation of the alternative pathway convertase C3bBb.⁴¹ From the SPR analysis and likely as a result of four potential C3b binding domains, both homodimeric mini-FH

constructs demonstrated avid binding profiles (Figure 3), in line with the expectation of dimeric therapeutic reagents.^{50,58} This fits with the successful functional dimerization of the constructs, with a size in the fluid phase of approximately 160 kD, *i.e.*, marginally bigger than full-length plasma purified FH.³⁸ SEC-MALS and classic size exclusion chromatography of purified constructs showed no evidence that monomeric or additional higher order constructs (Figure 1, Supplemental Figures 1 and 2) were generated during CHO cell production. Because the previously measured K_D values for the C3b::SCR 19–20 and C3b::SCR 1–4 interactions are in the ranges 3.4–7.8 μM ^{40,59,60} and 10.0–14.5 μM ,^{40,61} respectively, it is likely that at low concentrations of homodimeric mini-FH and on a densely deposited C3b surface, highly avid interactions with several C3b molecules occur, involving three to four homodimeric mini-FH C3b binding domains, increasing the potency of the drug. This is supported by the fluid C3b breakdown analysis and sheep erythrocyte protection assays, in which FH^{1-5^18-20^RI-2} consistently outperformed FH and FH^{1-5^18-20}. Interestingly, similar to FH^{1-5^18-20},^{40,43} the homodimeric constructs also readily bound iC3b and C3d, suggesting these molecules are in an “open” conformation as opposed to the “folded-back” or closed conformation of FH.^{14,54,62} This may be of great value. The homing of a therapeutic to the site of chronic complement activation may rely on the binding to a surface which has a high quantity of accumulated iC3b and C3d(g).^{63–65} On the negative side, this might present a risk of making these agents open to “sump” effects but, because the binding responses of the homodimeric mini-FH constructs to iC3b and C3d were significantly lower than compared with their binding to C3b-decorated surfaces (Figure 4B), this should be minimal.

Furthermore, because the crystal structures^{66–68} of C3b-FH imply that FH^{1-5^18-20} could bind to both GAGs and C3b (or iC3b/C3d[g]) simultaneously *via* three binding interfaces, regulation of surface binding by homodimeric mini-FH is going to be further modulated by the surface. This prediction is upheld by the *in vivo* studies as well as the sheep erythrocyte-based hemolysis assays, particularly for the C-terminal dimerized mini-FH, *i.e.*, FH^{1-5^18-20^RI-2}. This construct displays less avid binding on the SPR opsonized chip but displayed more potent decay accelerating and CFA

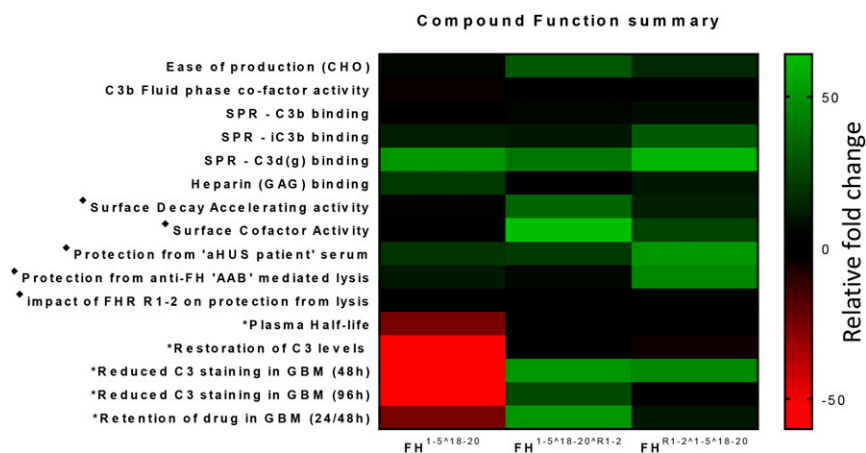


Figure 7. Review of functional attributes suggests the C-terminal dimerised version of HDM-FH is likely the most effective for treatment of C3G. Representative fold changes are colored from green (increased) to black (no change) to red (decreased), as indicated by the scale bar. ♦ on the basis of fold change in mean IC₅₀ in sheep red blood cell lysis assays. **In vivo* data collected from *Cfh*^{−/−} mice injected intraperitoneally with a single equimolar dose of homodimeric mini-FH or FH or a two-fold molar dose of FH^{1-5^18-20}. Heat Map columns and rows are labeled to identify the constructs and functions, respectively. AAB, autoantibody; aHUS, atypical hemolytic uremic syndrome; CHO, Chinese hamster ovary cells; GAG, glycosyl amino-glycan; GBM, glomerular basement membrane; SPR, surface plasmon resonance.

than the N-terminal dimerized mini-FH, *i.e.*, FH^{R1-2^1-5^18-20} (see Figure 7 for an overall functional comparison of the constructs). Thus, on the basis of the heparin/GAG binding, hemolysis, SPR, and *in vivo* studies, it is clear subtle differences in surface and C3 fragment interactions exist between the two homodimeric mini-FH constructs which culminate in unique functional profiles that ultimately may suit different *in vivo* situations.

The observed heterogeneity implies that homodimeric mini-FH binding to opsonized C3b surfaces is likely the result of a combination of high-affinity and low-affinity binding sites. This is potentially influenced by steric hindrance at sites adjacent to the dimerization domains linked to their glycosylation. The “link” regions between the FHR1 and FH SCRs were designed to be 9–10 amino acids long (from Cys to Cys), which is similar to “long” intermodular linkers found in FH,⁶⁹ and consisted as much as practical of natural linker sequence. That said, we cannot rule out that these engineered linker domains may be immunogenic in the context of the constructs and this theoretic risk for patients would have to be explored. Of course, we would expect such risks to be considerably lower than constructs generated in nonmammalian systems. The crosshybridization noted with FHR proteins might also present a small increased risk of infection through the complement regulatory potential of the FHR/dimeric mini-FH that might form in the blood stream when homodimeric mini-FH concentration drops in comparison to FHR1/2 levels. That said, the data on C3b-coated surfaces appear to suggest that homodimeric mini-FH would preferentially bind and

restore normal complement control at those sites. Further studies in the mouse, analyzing mouse homodimeric mini-FH constructs in the presence of mouse FHRs, may help address this question and are ongoing.

Thus, the intermodular linkers used in our homodimeric mini-FH constructs should allow a degree of inherent flexibility, although actual mobility may be constrained by the high binding affinity of the dimerization domains to each other and the glycosylation sites in this region.^{11,51,70} Under less flexible conditions, we can speculate that there remains potential for the two “arms” or component parts of the homodimeric mini-FH constructs to alternately anchor the molecule to the target surface in a homing fashion, allowing the “free-arm” to “patrol” an area adjacent to the C3b/GAGs that the first “arm” binds as well as rapidly recycling to other C3b molecules; this ability would be enhanced or restricted as a factor of the overall binding strength to the surface. An examination of “model patient” sera again highlights

how finely balanced this is, *i.e.*, FH^{1-5^18-20^R1-2} is less effective than FH^{R1-2^1-5^18-20} in counteracting the ability of anti-FH antibody and “hybrid protein”^{13,54} to deregulate alternative pathway activation. This implies that OX-24 binding to SCR 5 in FH^{R1-2^1-5^18-20} was obstructed, potentially, due to the proximity of the dimerization domain. Of course, FH^{1-5^18-20^R1-2} was still more effective than FH in the presence of OX-24 mAb, suggesting that it will work equally well or even better in patients with C3G with anti-FH because the autoantibodies associated with C3G are relatively low in affinity, don’t form immune complexes in circulation, and don’t perturb FH binding to its ligands,⁷¹ but clearly in this circumstance FH^{R1-2^1-5^18-20} would be better. Furthermore, in the case of the aHUS model serum (Figure 4C), where endogenous FH in the system has a C terminus equivalent to FHR1 (*i.e.*, the FH p.S1191A/p.V1197A molecule), FH^{R1-2^1-5^18-20} is 50-fold more potent than FH and 2.5-fold more potent than FH^{1-5^18-20} and FH^{1-5^18-20^R1-2} in the protection of red cells from hemolysis in the presence of a pathogenic variant, even in the presence of physiologic levels of FHR1/FHR2 (Figure 4E). Again, however, FH^{1-5^18-20^R1-2} is very effective compared with FH, suggesting on balance that this molecule is the better candidate drug in C3G (see Figure 7).

As demonstrated above and in other studies using modular regions of FH (*i.e.*, the mini-FH constructs,^{40–43,45} as well as TT30,⁷² a 56-kD fusion protein consisting of FH SCR 1–5 and complement receptor type 2 SCRs 1–4), concatenation of the complement regulator domain of FH to a complement break-down fragment targeting domain

dramatically increases *in vitro* alternative pathway regulatory efficacy.⁴¹ However, the majority of FH-based therapeutic molecules have a short *in vivo* plasma half-life. For example, CHO-produced recombinant human mini-FH or mouse CR2-FH were detectable for around 6 or 9 hours in serum after administered to *Cfh*^{-/-} mice, respectively,^{43,73} whereas plasma purified human FH was detectable for up to 2 days.³⁶ In man, human FH (from plasma infusion) was found to have a 6-day *t*_{1/2} in an FH-deficient patient.⁷⁴ Data on recombinant glycosylation-optimized full-length FH produced in moss and injected intravenously suggested serum *t*_{1/2} of minutes rather than hours.⁷⁵ In this context, both homodimeric mini-FH constructs possess markedly improved serum *t*_{1/2} compared with FH^{1-5^18-20^R1-2} (Figure 5A) and ability to restore plasma C3 levels. Thus, as with the *in vitro* fluid-phase assay, FH^{1-5^18-20^R1-2} was most effective in restoring normal complement function *in vivo*. Remarkably, FH^{1-5^18-20^R1-2} was able to completely restore the serum C3 level, surpassing the activity of FH, at the 24-hour time point. In addition to the improved efficacy in fluid phase, FH^{1-5^18-20^R1-2} was detected on the GBM colocalized with the C3 staining out to 48 hours, well beyond the other constructs or FH. This extended retention in the GBM was associated with a significant reduction in glomerular C3 staining at 96 hours or when using the much-reduced dose of the agent (0.375 nmol) at 48 hours (Figure 6, D and E, Supplemental Figure 8). The trajectory of C3 staining suggests it will return to pretreatment levels by 120 hours postapplication. This approaches the 120-hour residency time previously reported for mouse TT30.⁷³ However, in order to fully evaluate the true *in vivo* efficacy of these reagents, the mouse version of the HDM-FH molecules will be needed to better measure binding to murine C3 fragments/GAG/SAs and compete with mouse FHRs. This is now the subject of ongoing work.

In summary, our data strongly suggest that administration of FH^{1-5^18-20^R1-2} would be most appropriate in C3G, as a whole, due to marked improvement in both *in vitro* and *in vivo* functionality compared with mini-FH (FH^{1-5^18-20}). That is not to say that FH-based therapies will represent the only viable anticomplement therapy for use in C3G but their unique targeting nature and high avidity for those surfaces (particularly in the context of C3 deposition) make them an excellent option for consideration when compared with, for instance, total blockade of the terminal or alternative pathway of complement. Particularly, on the basis of this study, FH^{1-5^18-20^R1-2} would have utility to reregulate the complement system when endogenous FH is malfunctioning. We will also be assessing the functionality of these molecules in preventing the sequelae of ischemia reperfusion injury in human *in vitro* model systems, in order to establish their utility in other pathologic circumstances. In short, we are convinced that the homodimeric mini-FH molecules will provide viable therapeutic options to add to the anticomplement drug cabinet of the future.

ACKNOWLEDGMENTS

We thank the staff and technicians at Newcastle Bio-Imaging Facility and Comparative Biology Center for their help in conducting this study.

This study was funded by a Kidney Research UK project grant (RP7/2015) and Newcastle University (Medical Research Council of United Kingdom Confidence in Concept award). O.R.D. is a Sir Henry Dale Fellow jointly funded by the Wellcome Trust and Royal Society (grant number 104158/Z/14/Z). M.C.P. is a Wellcome Trust Senior Fellow in Clinical Science (fellowship WT082291MA).

DISCLOSURES

P.N.B. and K.J.M. are on the scientific advisory board of Gemini Therapeutics Inc. M.C.P. has received funding from Alexion Pharmaceuticals for pre-clinical studies of TT30 in *Cfh*^{-/-} mice and lecture fees.

REFERENCES

- Fakhouri F, Frémeaux-Bacchi V, Noël LH, Cook HT, Pickering MC: C3 glomerulopathy: A new classification. *Nat Rev Nephrol* 6: 494–499, 2010
- Xiao X, Pickering MC, Smith RJ: C3 glomerulopathy: The genetic and clinical findings in dense deposit disease and C3 glomerulonephritis. *Semin Thromb Hemost* 40: 465–471, 2014
- Pickering MC, D'Agati VD, Nester CM, Smith RJ, Haas M, Appel GB, et al.: C3 glomerulopathy: Consensus report. *Kidney Int* 84: 1079–1089, 2013
- Malik TH, Lavin PJ, Goicoechea de Jorge E, Vernon KA, Rose KL, Patel MP, et al.: A hybrid CFHR3-1 gene causes familial C3 glomerulopathy. *J Am Soc Nephrol* 23: 1155–1160, 2012
- Medjeral-Thomas N, Malik TH, Patel MP, Toth T, Terence Cook H, Tomson C, et al.: A novel CFHR5 fusion protein causes C3 glomerulopathy in a family without Cypriot ancestry. *Kidney Int* 85(4): 933–937, 2014
- Barbour TD, Pickering MC, Cook HT: Recent insights into C3 glomerulopathy. *Nephrol Dial Transplant* 28: 1685–1693, 2013
- Cook HT, Pickering MC: Histopathology of MPGN and C3 glomerulopathies. *Nat Rev Nephrol* 11: 14–22, 2015
- Gale DP, de Jorge EG, Cook HT, Martínez-Barricarte R, Hadjisavvas A, McLean AG, et al.: Identification of a mutation in complement factor H-related protein 5 in patients of Cypriot origin with glomerulonephritis. *Lancet* 376: 794–801, 2010
- Chen Q, Wiesener M, Eberhardt HU, Hartmann A, Uzonyi B, Kirschfink M, et al.: Complement factor H-related hybrid protein deregulates complement in dense deposit disease. *J Clin Invest* 124: 145–155, 2014
- Tortajada A, Yébenes H, Abarrategui-Garrido C, Anter J, García-Fernández JM, Martínez-Barricarte R, et al.: C3 glomerulopathy-associated CFHR1 mutation alters FHR oligomerization and complement regulation. *J Clin Invest* 123: 2434–2446, 2013
- Goicoechea de Jorge E, Caesar JJ, Malik TH, Patel M, Colledge M, Johnson S, et al.: Dimerization of complement factor H-related proteins modulates complement activation *in vivo*. *Proc Natl Acad Sci USA* 110: 4685–4690, 2013
- Józsi M: Factor H family proteins in complement evasion of microorganisms. *Front Immunol* 8: 571, 2017
- Józsi M, Tortajada A, Uzonyi B, Goicoechea de Jorge E, Rodríguez de Córdoba S: Factor H-related proteins determine complement-activating surfaces. *Trends Immunol* 36: 374–384, 2015

14. Makou E, Herbert AP, Barlow PN: Functional anatomy of complement factor H. *Biochemistry* 52: 3949–3962, 2013
15. Whaley K, Ruddy S: Modulation of the alternative complement pathways by beta 1 H globulin. *J Exp Med* 144: 1147–1163, 1976
16. Fenaille F, Le Mignon M, Groseil C, Ramon C, Riandé S, Siret L, et al.: Site-specific N-glycan characterization of human complement factor H. *Glycobiology* 17: 932–944, 2007
17. Weiler JM, Daha MR, Austen KF, Fearon DT: Control of the amplification convertase of complement by the plasma protein beta1H. *Proc Natl Acad Sci U S A* 73: 3268–3272, 1976
18. Fearon DT, Daha MR, Weiler JM, Austen KF: The natural modulation of the amplification phase of complement activation. *Transplant Rev* 32: 12–25, 1976
19. Gordon DL, Kaufman RM, Blackmore TK, Kwong J, Lublin DM: Identification of complement regulatory domains in human factor H. *J Immunol* 155: 348–356, 1995
20. Kühn S, Zipfel PF: Mapping of the domains required for decay acceleration activity of the human factor H-like protein 1 and factor H. *Eur J Immunol* 26: 2383–2387, 1996
21. Jokiranta TS, Zipfel PF, Hakulinen J, Kühn S, Pangburn MK, Tamerius JD, et al.: Analysis of the recognition mechanism of the alternative pathway of complement by monoclonal anti-factor H antibodies: Evidence for multiple interactions between H and surface bound C3b. *FEBS Lett* 393: 297–302, 1996
22. Blaum BS, Deakin JA, Johansson CM, Herbert AP, Barlow PN, Lyon M, et al.: Lysine and arginine side chains in glycosaminoglycan-protein complexes investigated by NMR, cross-linking, and mass spectrometry: A case study of the factor H-heparin interaction. *J Am Chem Soc* 132: 6374–6381, 2010
23. Morgan HP, Mertens HD, Guariento M, Schmidt CQ, Soares DC, Svergun DI, et al.: Structural analysis of the C-terminal region (modules 18–20) of complement regulator factor H (FH). *PLoS One* 7: e32187, 2012
24. Herbert AP, Kavanagh D, Johansson C, Morgan HP, Blaum BS, Hannan JP, et al.: Structural and functional characterization of the product of disease-related factor H gene conversion. *Biochemistry* 51: 1874–1884, 2012
25. Clark SJ, Perveen R, Hakobyan S, Morgan BP, Sim RB, Bishop PN, et al.: Impaired binding of the age-related macular degeneration-associated complement factor H 402H allotype to Bruch's membrane in human retina. *J Biol Chem* 285: 30192–30202, 2010
26. Clark SJ, Bishop PN, Day AJ: Complement factor H and age-related macular degeneration: The role of glycosaminoglycan recognition in disease pathology. *Biochem Soc Trans* 38: 1342–1348, 2010
27. Blaum BS, Hannan JP, Herbert AP, Kavanagh D, Uhrin D, Stehle T: Structural basis for sialic acid-mediated self-recognition by complement factor H. *Nat Chem Biol* 11: 77–82, 2015
28. Clark SJ, Ridge LA, Herbert AP, Hakobyan S, Mulloy B, Lennon R, et al.: Tissue-specific host recognition by complement factor H is mediated by differential activities of its glycosaminoglycan-binding regions. *J Immunol* 190: 2049–2057, 2013
29. Langford-Smith A, Day AJ, Bishop PN, Clark SJ: Complementing the sugar code: Role of GAGs and sialic acid in complement regulation. *Front Immunol* 6: 25, 2015
30. Pickering MC, Cook HT, Warren J, Bygrave AE, Moss J, Walport MJ, et al.: Uncontrolled C3 activation causes membranoproliferative glomerulonephritis in mice deficient in complement factor H. *Nat Genet* 31: 424–428, 2002
31. Pickering MC, Warren J, Rose KL, Carlucci F, Wang Y, Walport MJ, et al.: Prevention of C5 activation ameliorates spontaneous and experimental glomerulonephritis in factor H-deficient mice. *Proc Natl Acad Sci U S A* 103: 9649–9654, 2006
32. Herlitz LC, Bomback AS, Markowitz GS, Stokes MB, Smith RN, Colvin RB, et al.: Pathology after eculizumab in dense deposit disease and C3 GN. *J Am Soc Nephrol* 23: 1229–1237, 2012
33. Bomback AS, Smith RJ, Barile GR, Zhang Y, Heher EC, Herlitz L, et al.: Eculizumab for dense deposit disease and C3 glomerulonephritis. *Clin J Am Soc Nephrol* 7: 748–756, 2012
34. Harris CL: Expanding horizons in complement drug discovery: Challenges and emerging strategies. *Semin Immunopathol* 40(1): 125–140, 2018
35. Paixão-Cavalcante D, Hanson S, Botto M, Cook HT, Pickering MC: Factor H facilitates the clearance of GBM bound iC3b by controlling C3 activation in fluid phase. *Mol Immunol* 46: 1942–1950, 2009
36. Fakhouri F, de Jorge EG, Brune F, Azam P, Cook HT, Pickering MC: Treatment with human complement factor H rapidly reverses renal complement deposition in factor H-deficient mice. *Kidney Int* 78: 279–286, 2010
37. Sharma AK, Pangburn MK: Biologically active recombinant human complement factor H: Synthesis and secretion by the baculovirus system. *Gene* 143: 301–302, 1994
38. Schmidt CQ, Slingsby FC, Richards A, Barlow PN: Production of biologically active complement factor H in therapeutically useful quantities. *Protein Expr Purif* 76: 254–263, 2011
39. Büttner-Mainik A, Parsons J, Jérôme H, Hartmann A, Lamer S, Schaaf A, et al.: Production of biologically active recombinant human factor H in *Physcomitrella*. *Plant Biotechnol J* 9: 373–383, 2011
40. Schmidt CQ, Bai H, Lin Z, Risitano AM, Barlow PN, Ricklin D, et al.: Rational engineering of a minimized immune inhibitor with unique triple-targeting properties. *J Immunol* 190: 5712–5721, 2013
41. Schmidt CQ, Harder MJ, Nichols EM, Hebecker M, Anliker M, Höchsmann B, et al.: Selectivity of C3-opsonin targeted complement inhibitors: A distinct advantage in the protection of erythrocytes from paroxysmal nocturnal hemoglobinuria patients. *Immunobiology* 221: 503–511, 2016
42. Hebecker M, Alba-Domínguez M, Roumenina LT, Reuter S, Hyvärinen S, Dragon-Durey MA, et al.: An engineered construct combining complement regulatory and surface-recognition domains represents a minimal-size functional factor H. *J Immunol* 191: 912–921, 2013
43. Nichols EM, Barbour TD, Pappworth IY, Wong EK, Palmer JM, Sheerin NS, et al.: An extended mini-complement factor H molecule ameliorates experimental C3 glomerulopathy. *Kidney Int* 88: 1314–1322, 2015
44. Harder MJ, Anliker M, Reis ES, Huber-Lang M, Schrezenmeier H, Höchsmann B, et al.: Evaluation of factor H (FH), miniFH and the Fc-fusion protein Fc-miniFH in pharmacokinetic studies and different in vitro models of complement mediated diseases. *Immunobiology* 221: 1217–1218, 2016
45. Harder MJ, Anliker M, Höchsmann B, Simmet T, Huber-Lang M, Schrezenmeier H, et al.: Comparative analysis of novel complement-targeted inhibitors, MiniFH, and the natural regulators factor H and factor H-like protein 1 reveal functional determinants of complement regulation. *J Immunol* 196: 866–876, 2016
46. Harding SE, Jumel K: Light scattering. *Curr Protoc Protein Sci* Chapter 11: Unit 7.8, 7.8.1–7.8.14, 2001
47. Harris CL, Abbott RJ, Smith RA, Morgan BP, Lea SM: Molecular dissection of interactions between components of the alternative pathway of complement and decay accelerating factor (CD55). *J Biol Chem* 280: 2569–2578, 2005
48. Tortajada A, Montes T, Martínez-Barricarte R, Morgan BP, Harris CL, de Córdoba SR: The disease-protective complement factor H allotypic variant Ile62 shows increased binding affinity for C3b and enhanced cofactor activity. *Hum Mol Genet* 18: 3452–3461, 2009
49. Jönsson U, Fägerstam L, Ivarsson B, Johnsson B, Karlsson R, Lundh K, et al.: Real-time biospecific interaction analysis using surface plasmon resonance and a sensor chip technology. *Biotechniques* 11: 620–627, 1991
50. Harris CL, Hughes CE, Williams AS, Goodfellow I, Evans DJ, Caterson B, et al.: Generation of anti-complement “prodrugs”: Cleavable reagents for specific delivery of complement regulators to disease sites. *J Biol Chem* 278: 36068–36076, 2003

51. Skerka C, Horstmann RD, Zipfel PF: Molecular cloning of a human serum protein structurally related to complement factor H. *J Biol Chem* 266: 12015–12020, 1991
52. van Beek AE, Pouw RB, Brouwer MC, van Mierlo G, Geissler J, Ooijevaar-de Heer P, et al.: Factor H-Related (FHR)-1 and FHR-2 form homo- and heterodimers, while FHR-5 circulates only as homodimer in human plasma. *Front Immunol* 8: 1328, 2017
53. Harris CL, Pettigrew DM, Lea SM, Morgan BP: Decay-accelerating factor must bind both components of the complement alternative pathway C3 convertase to mediate efficient decay. *J Immunol* 178: 352–359, 2007
54. Kerr H, Wong E, Makou E, Yang Y, Marchbank K, Kavanagh D, et al.: Disease-linked mutations in factor H reveal pivotal role of cofactor activity in self-surface-selective regulation of complement activation. *J Biol Chem* 292: 13345–13360, 2017
55. Herbert AP, Makou E, Chen ZA, Kerr H, Richards A, Rappsilber J, et al.: Complement evasion mediated by enhancement of captured factor H: Implications for protection of self-surfaces from complement. *J Immunol* 195: 4986–4998, 2015
56. Goodship TH, Pappworth IY, Toth T, Denton M, Houlberg K, McCormick F, et al.: Factor H autoantibodies in membranoproliferative glomerulonephritis. *Mol Immunol* 52: 200–206, 2012
57. Moore I, Strain L, Pappworth I, Kavanagh D, Barlow PN, Herbert AP, et al.: Association of factor H autoantibodies with deletions of CFHR1, CFHR3, CFHR4, and with mutations in CFH, CFI, CD46, and C3 in patients with atypical hemolytic uremic syndrome. *Blood* 115: 379–387, 2010
58. Vauquelin G, Charlton SJ: Exploring avidity: Understanding the potential gains in functional affinity and target residence time of bivalent and heterobivalent ligands. *Br J Pharmacol* 168: 1771–1785, 2013
59. Schmidt CQ, Herbert AP, Kavanagh D, Gandy C, Fenton CJ, Blaum BS, et al.: A new map of glycosaminoglycan and C3b binding sites on factor H. *J Immunol* 181: 2610–2619, 2008
60. Jokiranta TS, Jaakola VP, Lehtinen MJ, Pärepa M, Meri S, Goldman A: Structure of complement factor H carboxyl-terminus reveals molecular basis of atypical haemolytic uremic syndrome. *EMBO J* 25: 1784–1794, 2006
61. Pecht IC, Kavanagh D, McIntosh N, Harris CL, Barlow PN: Disease-associated N-terminal complement factor H mutations perturb cofactor and decay-accelerating activities. *J Biol Chem* 286: 11082–11090, 2011
62. Okemefuna AI, Nan R, Gor J, Perkins SJ: Electrostatic interactions contribute to the folded-back conformation of wild type human factor H. *J Mol Biol* 391: 98–118, 2009
63. Huang Y, Qiao F, Atkinson C, Holers VM, Tomlinson S: A novel targeted inhibitor of the alternative pathway of complement and its therapeutic application in ischemia/reperfusion injury. *J Immunol* 181: 8068–8076, 2008
64. Holers VM, Rohrer B, Tomlinson S: CR2-mediated targeting of complement inhibitors: Bench-to-bedside using a novel strategy for site-specific complement modulation. *Adv Exp Med Biol* 735: 137–154, 2013
65. Ruseva MM, Ramaglia V, Morgan BP, Harris CL: An anticomplement agent that homes to the damaged brain and promotes recovery after traumatic brain injury in mice. *Proc Natl Acad Sci U S A* 112: 14319–14324, 2015
66. Xue X, Wu J, Ricklin D, Forneris F, Di Crescenzo P, Schmidt CQ, et al.: Regulator-dependent mechanisms of C3b processing by factor I allow differentiation of immune responses. *Nat Struct Mol Biol* 24: 643–651, 2017
67. Morgan HP, Schmidt CQ, Guariento M, Blaum BS, Gillespie D, Herbert AP, et al.: Structural basis for engagement by complement factor H of C3b on a self surface. *Nat Struct Mol Biol* 18: 463–470, 2011
68. Wu J, Wu YQ, Ricklin D, Janssen BJ, Lambris JD, Gros P: Structure of complement fragment C3b-factor H and implications for host protection by complement regulators. *Nat Immunol* 10: 728–733, 2009
69. Makou E, Mertens HD, Maciejewski M, Soares DC, Matis I, Schmidt CQ, et al.: Solution structure of CCP modules 10–12 illuminates functional architecture of the complement regulator, factor H. *J Mol Biol* 424: 295–312, 2012
70. Solá RJ, Griebenow K: Effects of glycosylation on the stability of protein pharmaceuticals. *J Pharm Sci* 98: 1223–1245, 2009
71. Blanc C, Togarsimalemath SK, Chauvet S, Le Quintrec M, Moulin B, Buchler M, et al.: Anti-factor H autoantibodies in C3 glomerulopathies and in atypical hemolytic uremic syndrome: One target, two diseases. *J Immunol* 194: 5129–5138, 2015
72. Fridkis-Hareli M, Storek M, Mazsaroff I, Risitano AM, Lundberg AS, Horvath CJ, et al.: Design and development of TT30, a novel C3d-targeted C3/C5 convertase inhibitor for treatment of human complement alternative pathway-mediated diseases. *Blood* 118: 4705–4713, 2011
73. Ruseva MM, Peng T, Lasaro MA, Bouchard K, Liu-Chen S, Sun F, et al.: Efficacy of targeted complement inhibition in experimental C3 glomerulopathy. *J Am Soc Nephrol* 27: 405–416, 2016
74. Licht C, Weyersberg A, Heinen S, Stapenhorst L, Devenge J, Beck B, et al.: Successful plasma therapy for atypical hemolytic uremic syndrome caused by factor H deficiency owing to a novel mutation in the complement cofactor protein domain 15. *Am J Kidney Dis* 45: 415–421, 2005
75. Michelfelder S, Parsons J, Bohlender LL, Hoernstein SNW, Niederkrüger H, Busch A, et al.: Moss-produced, glycosylation-optimized human factor H for therapeutic application in complement disorders. *J Am Soc Nephrol* 28: 1462–1474, 2017

This article contains supplemental material online at <http://jasn.asnjournals.org/lookup/suppl/doi:10.1681/ASN.2017091006/-/DCSupplemental>.